CORA Cork Open Research Archive
Cartlann Taighde Oscailte Chorcaí

UCC Library and UCC researchers have made this item openly available. Please let us know how this has helped you. Thanks!

Title	Investigation of calmodulinlike and rod domain mutations suggests common molecular mechanism for αactinin1linked congenital macrothrombocytopenia
Author(s)	O'Sullivan, Leanne Rose; Ajaykumar, Praburam Amarendra; Dembicka, Kornelia Maria; Murphy, Aidan; Grennan, Eamonn Paul; Young, Paul W.
Publication date	2019-07-31
Original citation	O'Sullivan, L. R., Ajaykumar, P. A., Dembicka, K. M., Murphy, A., Grennan, E. P. and Young, P. W. (2019) 'Investigation of calmodulinlike and rod domain mutations suggests common molecular mechanism for α actinin1linked congenital macrothrombocytopenia', FEBS Letters. doi: 10.1002/1873-3468.13562
Type of publication	Article (peer-reviewed)
Link to publisher's version	https://febs.onlinelibrary.wiley.com/doi/abs/10.1002/1873-3468.13562 http://dx.doi.org/10.1002/1873-3468.13562 Access to the full text of the published version may require a subscription.
Rights	**© 2019, Federation of European Biochemical Societies. Published by John Wiley & Sons, Inc. This is the peer reviewed version of the following article: O'Sullivan, L. R., Ajaykumar, P. A., Dembicka, K. M., Murphy, A., Grennan, E. P. and Young, P. W. (2019) 'Investigation of calmodulin-like and rod domain mutations suggests common molecular mechanism for α-actinin-1-linked congenital macrothrombocytopenia', FEBS Letters. doi: 10.1002/1873-3468.13562, which has been published in final form at https://doi.org/10.1002/1873-3468.13562. This article may be used for non-commercial purposes in accordance with Wiley Terms and Conditions for Use of Self-Archived Versions.**
Embargo information	Access to this article is restricted until 12 months after publication by request of the publisher.
Embargo lift date	2020-07-31
Item downloaded from	http://hdl.handle.net/10468/8505

Downloaded on 2021-11-27T07:16:00Z
University College Cork, Ireland
Coláiste na hOllscoile Corcaigh

DR. PAUL WILLIAM YOUNG (Orcid ID : 0000-0002-1307-0249)

Received Date : 31-May-2019

Revised Date : 22-Jul-2019

Accepted Date : 29-Jul-2019

Article type : Research Letter

Investigation of calmodulin-like and rod domain mutations suggests common molecular mechanism for α-actinin-1-linked congenital macrothrombocytopenia

Leanne Rose O'Sullivan, Amarendra Praburam Ajaykumar, Kornelia Maria Dembicka, Aidan Murphy, Eamonn Paul Grennan and Paul William Young†

School of Biochemistry and Cell Biology, Western Gateway Building, University College Cork, Cork, Ireland

† Corresponding author

Contact details:

Western Gateway Building Room: 3.42

School of Biochemistry and Cell Biology,
Western Road
University College Cork,
Cork, Ireland
Email: p.young@ucc.ie
Telephone: +353 21 420 5994
FAX: +353 21 420 5462

This article has been accepted for publication and undergone full peer review but has not been through the copyediting, typesetting, pagination and proofreading process, which may lead to differences between this version and the Version of Record. Please cite this article as doi: 10.1002/1873-3468.13562

This article is protected by copyright. All rights reserved.

Accepted Article

Keywords:
Actin, alpha-actinin, α-actinin, ACTN1, actinin-1, macrothrombocytopenia, congenital macrothrombocytopenia

Short title:
Macrothrombocytopenia-causing actinin-1 mutations

Highlights:

- Biochemical analysis of congenital macrothrombocytopenia causing actinin-1 mutations
- Calcium binding not consistently affected by CaM-like domain mutations
- Mutations within the rod and CaM-like domains increase actinin-1 association with F-actin
- Similar effect to previously described mutations in the actinin-1 actin binding domain
- Suggests a common molecular mechanism for most disease-associated actinin-1 mutations

Abstract

Actinin-1 mutations cause dominantly-inherited congenital macrothrombocytopenia (CMTP), with mutations in the actin-binding domain increasing actinin's affinity for F-actin. In this study, we examined nine CMTP-causing mutations in the calmodulin-like and rod domains of actinin-1. These mutations increase, to varying degrees, actinin's ability to bundle actin filaments *in vitro*. Mutations within the calmodulin-like domain decrease its thermal stability slightly but do not dramatically affect calcium binding, with mutant proteins retaining calcium-dependent regulation of filament bundling *in vitro*. The G764S and E769K mutations increase cytoskeletal association of actinin in cells, and all mutant proteins colocalize with F-actin in cultured HeLa cells. Thus, CMTP-causing actinin-1 mutations outside the actin-binding domain also increase actin association, suggesting a common molecular mechanism underlying actinin-1 related CMTP.

This article is protected by copyright. All rights reserved.

Accepted Article

Introduction

α-Actinins (actinins) are actin-binding proteins which exist as antiparallel dimers consisting of an actin-binding domain (ABD), a carboxyl-terminal, calcium-binding calmodulin-like (CaM-like) domain and a central rod region (Fig. 1) [1].The rod domain mediates actinin dimerization and is comprised of four spectrin-like repeats (SR1-SR4) which connect the amino- and carboxyl-terminal domains [2,3]. Actinin cross-links actin filaments, with major functions in cytokinesis, cell motility and adhesion [4,5]. The CaM-like domain comprises two pairs of EF hand motifs (EF1-2 and EF3-4) and in the non-muscle isoform of actinin-1 calcium binding to EF1 inhibits binding and cross-linking of actin filaments. The recently described structure of the actinin-1 CaM-like domain suggests that the binding of a single calcium ion to EF1 facilitates a restructuring of the EF3-4 region to a more open conformation, stabilising its binding to the "neck" region adjacent to the ABD of the opposing subunit and thereby regulating actinin's interaction with F-actin [6].

The platelet disorder congenital macrothrombocytopenia (CMTP) is characterised by a low platelet count (<150 x10^9 cells / L) and large platelet size resulting in a heightened bleeding risk of varying severity [7]. Recently described mutations in actinin-1 are thought to contribute to 5% of CMTP cases, making it the fourth most common cause of this disease [8,9]. To date, at least 37 likely CMTP-causing mutations in actinin-1 have been identified, with mutations in all of the functional domains having been described [8,10–17]. The residues mutated in actinin-1 linked CMTP are conserved in other actinin isoforms (actinin-2, -3 and -4) and hence are likely to have importance for all actinin isoforms [18]. CMTP-associated mutations in the actinin-1 ABD have been demonstrated to increase its affinity for F-actin, a molecular mechanism common to the inherited kidney disorder, focal and segmented glomerulosclerosis (FSGS) that is caused by actinin-4 mutations [19,20]. The consequences of mutations in the rod and CaM-like domain have not been examined at a molecular level.

Although actinin-1 is widely expressed and has a broad range of cellular functions, it appears that actinin-1 mutations have consequences only in platelets [8], implying a tissue-specific role. Actinin-1 was first identified in platelets as being a prominent component of the platelet cytoskeleton [21,22].

This article is protected by copyright. All rights reserved.

Accepted Article

Accepted Article

Genome wide association studies (GWAS) have implicated actinin-1 in platelet parameters including platelet size and platelet count indicating they play a role in platelet formation [23–25]. Actinin-1 has an important role in cytokinesis, and has been implicated in endomitosis in megakaryocytes, the process whereby a failure of cytokinesis creates polyploid cells [26,27]. At later stages of platelet production, megakaryocytes display extension of cytoplasmic processes with platelet-sized buds, termed proplatelet tips, which are released into the vasculature [28]. Mutant actinin-1 proteins were shown to diminish the number of proplatelet tips and increase their size in an *in vitro* study [12]. However, analysis of megakaryocytes from affected individuals suggested proplatelet production was active but cells displayed large granules and the cytoplasm showed disorganisation [13]. Actinin-1 also plays important roles during platelet activation and can associate with other platelet activation components including integrin $\alpha IIb\beta_3$, GpIb-IX-V, integrin β_2 and signalling intermediates PI3K and PKN [29–33]. However, platelets isolated from individuals affected with actinin-1 related CMTP are functionally normal in terms of platelet activation [11,12]. Hence the molecular mechanisms underlying actinin-1 related CMTP have yet to be fully defined.

In this study, we tested the hypothesis that CMTP-causing mutations in the CaM-like domain might affect calcium binding and, thus, the regulation of actinin-1's association with F-actin. However, we find that calcium binding is not consistently compromised and rather that actin-bundling ability *in vitro* and association with F-actin in cells is enhanced for three CaM-like domain mutations examined. In addition, we show that mutations in the rod domain can also enhance actin bundling ability *in vitro*. This gain of function phenotype is very similar to that seen for mutations affecting the ABD [20]. Hence, a common molecular mechanism appears to exist for most actinin-1 mutations implicated in CMTP, regardless of the affected protein domain.

Materials & Methods

Actinin-1 cDNA constructs

The calcium-sensitive (non-muscle, exon 19a-containing) splice variant of human actinin-1 was used in all experiments (Accession no. NM_001102). Wild type (WT) and mutant actinin-1 constructs for both bacterial and mammalian expression were prepared as described previously [20]. Constructs to produce the isolated WT and mutant CaM-like

This article is protected by copyright. All rights reserved.

domain encoded amino acids 740-892 of actinin-1 with an additional three amino acids (Gly-Ser-Ser) at the amino terminus.

Protein expression & purification

Protein expression and removal of affinity tags was performed as described previously [20] except that an additional size exclusion chromatography step was performed using a Superdex 75 10/300 GL column for CaM-like domain constructs and a Superdex 200 10/300 GL column for full-length actinin proteins on an AKTA Purifier 10 Fast Protein Liquid Chromatography system (GE Amersham). Proteins were eluted in filtered and degassed 100 mM NaCl, 20 mM HEPES pH 7.5 for CaM-like domains and 10 mM Tris pH7.5, 100 mM NaCl, 0.1 mM DTT for full length actinin proteins. When necessary, proteins were concentrated using Amicon Ultra-4 Centrifugal Filters (Merck). For isothermal calorimetry and thermal shift assays, proteins were treated with Chelex-100 calcium binding resin (Sigma-Aldrich) for 2 - 16 hours at 4 °C prior to analysis.

Thermal shift assays

Purified actinin-1 CaM-like domain protein (20 µM) was mixed with Sypro Orange dye (Sigma-Aldrich, S5692, used at a 1:250 dilution) in either the presence or absence of 1 mM $CaCl_2$. Samples were heated across a temperature range from 25 to 95 °C with a rate of change in temperature of 1 °C/ min in a StepOne Plus Real Time PCR System (Applied Biosystems) while recording fluorescence at 1 min intervals using ROX Dye filter setting (Excitation at 488 nm with detection using a 615/30 nm band pass filter). The fluorescence emission signal was plotted against temperature using Microsoft Excel software and an average plot was deduced for each protein. The melting temperature (T_m) of each protein in the presence and absence of $CaCl_2$ was then deduced from a plot of minus the first derivative of fluorescence emission with respect to temperature, with the lowest point on this curve representing the T_m.

Isothermal calorimetry

Calcium binding efficiency was assessed with the Microcal PEAQ-ITC isothermal calorimeter (Malvern Panalytical) using purified actinin-1 CaM-like domains. 160-200 µM CaM-like domain protein in reaction buffer (100 mM NaCl, 20 mM HEPES pH 7.5) was loaded into the reaction chamber. $CaCl_2$ was added to reaction chamber in 19 sequential 2 µL injections, with an initial small

This article is protected by copyright. All rights reserved.

injection of 0.4 µL (4 seconds per injection), at 150 second intervals, and an initial delay of 60 seconds, from a reservoir of 8 mM $CaCl_2$ in identical reaction buffer. The reference cell contained reaction buffer. Heat change was monitored from a baseline of 25 °C relative to increase in calcium: protein molar ratio. Sample results were analysed following subtraction of heat of dilution, which was obtained by measuring heat change when $CaCl_2$ was added to reaction buffer without protein, using the same injection protocol. Dissociation constant (K_d), molar ratio of ligand to target (N), heat change (ΔH) and free energy change (ΔG) were calculated using Microcal PEAQ-ITC Analysis software (Malvern Panalytical).

Actin co-sedimentation assays

Actin co-sedimentation assays were performed essentially as previously reported [20,34] and are described as Supplementary Material accompanying this paper.

Cytoskeletal purification assays

Purification of cytoskeletal fractions from HeLa cells was carried out largely as previously described [20,35], but a detailed description is provided as Supplementary Material.

Immunofluorescence studies

Sterile glass cover slips were air-dried in 6-well plates and coated with poly-L-lysine by incubation at room temperature for 1 hour, followed by rinsing with sterile PBS. HeLa cells (0.2×10^6 cells per well) were plated onto sterile cover slips and grown at 37 °C until 60% confluent. Transfection was carried out as described for cytoskeletal purification assays, using 2 µg Actinin-1-GFP plasmid. 36 hours post transfection, cover slips were rinsed twice in PBS and fixed in 4% paraformaldehyde (PFA) on ice for 10 minutes. Coverslips were then rinsed again with PBS and blocked for 30 minutes at room temperature with blocking solution (5% normal goat serum, 2% BSA, 0.2% Triton). Following blocking and rinsing again in PBS, coverslips were stained with rhodamine phalloidin (1:3000) and DAPI (1:10,000) in blocking buffer without Triton for 1 hour at room temperature and then rinsed again with PBS. Coverslips were mounted on glass slides using Fluoromount (Sigma) and edges of coverslips were sealed with varnish. Images were acquired on a Leica DM6000 upright fluorescence microscope. Analysis of the width of bundled actin fibres was performed by a

This article is protected by copyright. All rights reserved.

Accepted Article

researcher who was blinded to the identity of the transfected actinin proteins. Measurements of 2-4 phalloidin stained actin fibres in 5-7 cells per mutant protein were made using ImageJ software [36]. Local thresholding was performed for each fibre and a fibre segment 2-10 μm long was defined using the "analyse particles" function. Measurements of the area and length (taken as the Feret diameter) were made and the area divided by the length was used to calculate the average fibre width.

Statistical analysis

Statistical analysis was carried out using SPSS data analysis software (IBM).

Results

Actinin-1 CaM-like domains with CMTP-causing mutations have decreased thermal stability but maintain calcium binding ability.

Three CMTP-linked mutations (R752Q, G764S and E769K) are located within the calcium-binding EF1 region of the CaM-like domain of actinin-1. R752Q is positioned in the middle of the first helix away from the calcium-binding site whereas both G764S and E769K are adjacent to residues directly involved in coordination of calcium (Supplemental Fig. 1B). As a first step in the functional characterization of these mutations we examined the thermal stability of the isolated CaM-like domain using a thermal shift assay in which increased fluorescence of Sypro Orange dye gives a readout of protein unfolding. In this assay both the WT and mutant proteins exhibited an unexpectedly high initial fluorescence signal that trended downwards as the temperature increased from 25 to approximately 55 °C (Fig. 2A). This is possibly due to loose association between the dye and hydrophobic regions of the CaM-like domain. Nevertheless, as the temperature climbed above 60 °C, a clear peak in fluorescence is observed that we interpret as corresponding to unfolding of the CaM-like domain, with increased Sypro Orange binding initially and its subsequent dissociation as the protein aggregates (Fig. 2B). This interpretation is supported by the observation that this peak is shifted to the right in the presence of calcium, which would be expected to stabilize the CaM-like domain.

This article is protected by copyright. All rights reserved.

Accepted Article

Melting temperatures (T_m) for WT and mutant CaM-like domains in the presence and absence of calcium were determined from a plot of minus the first derivative of fluorescence emission with respect to temperature (Fig. 2C). The T_m values of the mutant proteins were somewhat lower than the WT, both in the absence and presence of calcium (Fig. 2D). These differences were statistically significant for the G764S and E769K mutants, implying that these mutants are less thermally stable than the WT protein. Examining each individual protein in the presence and absence of calcium we found that T_m was significantly increased for all proteins in the presence of calcium, however while the extent of this increase was 8-10 °C for the WT, R752Q, G764S proteins it was only 4 °C for the E769K mutant. Thus, while some small differences in their thermal stability was observed, all the mutant proteins are capable of binding calcium.

Calcium binding affinity of actinin-1 CaM-like domains is not dramatically affected by the G764S and R752Q CMTP-causing mutations.

While thermal shift assays indicated that CaM-like domains with the R752Q, G764S and E769K mutations retained their ability to bind calcium it is possible that they differ quantitatively from the WT protein in their calcium binding affinity. We therefore employed isothermal calorimetry to quantitatively assess calcium binding of WT and mutant actinin-1 CaM-like domain proteins. The thermogram for the WT CaM-like domain protein shows a single endothermic event (Fig. 3A). The binding stoichiometry (N) of 0.96 ± 0.15 for the WT protein implies a single binding event per CaM-like domain molecule, and the calculated K_d of 114.94 ± 15.20 μM (Table 1) is in line with previous reports [6,37]. Melting profiles for G764S and R752Q proteins appeared similar to the WT and the calculated K_d and N values are also comparable, although variability between experimental replicates was somewhat greater than for the WT protein (Fig. 3B and 3C, Table 1). Hence calcium binding efficiency appears largely unaffected in the G764S and R752Q mutants. Thermograms for the E769K mutant differed substantially however, exhibiting DP and ΔH values that are approximately 10-fold lower than for the other proteins (Fig. 3D). Results from experimental replicates with different batches of E769K protein were highly variable which precluded the accurate calculation of binding parameters for this mutant.

This article is protected by copyright. All rights reserved.

Accepted Article

Accepted Article

CMTP-causing mutations in the rod and CaM-like domain enhance the F-actin bundling ability of actinin-1

We next assessed the ability of full-length actinin-1 proteins with mutations in the CaM-like domain to bundle actin filaments in co-sedimentation assays. We also examined proteins with the R738W mutation at the very end of SR4 and the L395Q mutation within SR2 of the rod domain (Supplemental Fig. 1C). Analysing levels of actin and actinin-1 in the supernatants and pellets from these assays (Fig. 4A) it is apparent that the WT and all mutant actinin-1 proteins are able to bind to (Fig. 4B), and bundle (Fig. 4C) actin filaments in the absence of calcium. These abilities are significantly decreased in the presence of calcium for all proteins implying that calcium sensitivity is maintained in full-length actinin-1 proteins harbouring CMTP-causing mutations. Examining actin bundling in the absence of calcium it was found that all the mutant proteins assessed had a greater ability to bundle actin than WT actinin-1 (Fig. 4C). This was statistically significant for one rod (L395Q), and two CaM-like domain (R752Q and E769K) mutations. By comparison, while the levels of bound actinin were generally higher for the mutants compared to the WT this was not statistically significant for any of the mutant proteins (Fig. 4B).

The observation that mutations in the CaM-like and rod domains affect actin binding/bundling in a similar manner to ABD mutations is somewhat surprising, especially for the L395Q mutation given its location in the middle of the central rod domain. This suggests that enhanced actin binding/bundling might be common to all CMTP-linked actinin-1 mutations and that actin bundling might be a functional assay that could distinguish pathogenic mutations from those of uncertain significance. We therefore assessed actin bundling for another four rod domain mutations. These included R320Q and L547P, located in SR1 and SR3 respectively, which are classified as likely pathogenic[16]. We also assessed two mutations of the same residue, one of which (T737N) is likely pathogenic [16,38], and the other (T737S) that was deemed to be a variant of unknown significance[8]. The R320Q, T737N and T737S mutant proteins all show a highly significant increase in actin bundling activity whereas a much smaller and not statistically significant increase was seen for L547P (Fig. 4D-4F). These findings indicate that mutations throughout the rod domain can affect actin binding properties, albeit to varying extents, and that relatively conservative amino acid substitutions such as T737S can nevertheless have functional consequences.

This article is protected by copyright. All rights reserved.

Accepted Article

CMTP-causing mutations in the CaM-like domain of actinin-1 increase the stability of its association with the actin cytoskeleton in cells.

To assess if the increased actin-bundling of the CaM-like domain and rod domain mutants was evident *in-cellula*, the association of FLAG-tagged actinin-1 with F-actin in cytoskeletal fractions purified from cultured HeLa cells was examined for the L395Q, G764S and E769K mutations. Significantly increased actinin-1 in cytoskeletal fractions was observed for the two CaM-like domain mutations (G764S and E769K) compared to the WT protein (Fig. 5A), whereas an increase for rod domain mutation L395Q was very slight and not statistically significant.

It has been reported that actinin-1 proteins with CMTP-linked mutations can disrupt the actin cytoskeleton and have an altered distribution in the cytosol of cultured megakaryocytes, human fibroblasts and CHO cells [8,10–13,17] whereas we did not find this to be the case in HeLa cells for FLAG-tagged proteins with mutations in the ABD for example [20]. To further examine this issue we transiently expressed WT GFP-tagged actinin-1 as well as two mutants affecting the ABD (V105I and E225K), two affecting the rod domain (L395Q and R738W) and three affecting the CaM-like domain (R752Q, G764S and E769K) in HeLa cells (Fig. 5C). We then examined the localization of actinin-GFP in relation to the F-actin cytoskeleton. The majority of transfected HeLa cells could not be distinguished from untransfected cells in terms of F-actin organization and consistent co-localization of both WT and all mutant actinin-1-GFP proteins with F-actin was observed, both in HeLa cells (Fig. 5C) and differentiating MEG-01 megakaryoblast cells (Supplemental Fig. 2). Quantification of the diameters of bundled actin fibres in HeLa cells did not reveal significant differences between cells expressing WT and mutant actinin-1 proteins (Fig. 5D), in contrast to a recent report using CHO cells for different CMTP-linked actinin-1 mutations [17]. Our findings suggest that, at least in HeLa cells, the mutant actinin-1 proteins examined here retain their association with F-actin and do not dramatically affect cytoskeletal organization.

This article is protected by copyright. All rights reserved.

Accepted Article

Discussion

We previously demonstrated that CMTP-linked mutations in actinin-1 that occur in the ABD increase the protein's affinity for and cross-linking of actin filaments [20]. Here, we have extended this analysis focusing on mutations in CaM-like and rod domains to ascertain whether they have similar effects on actin binding properties.

Mutations in the CaM-like domain

Three amino acids mutated in actinin-1-linked CMTP map to EF1 of the CaM-like domain, the only EF hand motif in actinin-1 that is functional in terms of calcium binding. R752Q or R752P mutations have been reported in four families [8,11,12,16] while the G764S and E769K mutations have each been reported in a single family to date[11]. Calcium binding to EF1 is thought to cause structural stabilisation of the CaM-like domain of actinin-1 with a more open conformation of EF3-4 promoting its interaction with the neck region adjacent to the ABD of the opposing subunit in the actinin dimer and consequently impairing actinin's ability to cross link F-actin, due to increased rigidity in the neck region [6].

Thermal shift assays allowed us to examine the effects of CMTP-linked mutations on both the stability and calcium binding ability of the isolated CaM-like domain. We observed high levels of fluorescence at room temperature for both the WT and mutant CaM-like domain in these assays(Fig. 2A). This may be due to factors such as the lack of a compact globular shape or the presence of exposed hydrophobic regions in a protein and has been reported to occur in 15-25% recombinant proteins [39,40]. Nevertheless, a peak in fluorescence that was observed for the WT protein as the temperature rose above 60 °C could be interpreted as corresponding to the thermal denaturation of the CaM-like domain on the basis that (1) it was shifted to the right in the presence of calcium (but not magnesium; data not shown) and (2) the observed T_m values of 74.8 and 85.1 °C in the absence and presence of calcium are in line with the high melting temperatures that have been reported for calmodulin and related EF-hand-containing proteins [41,42]. The T_m values for CaM-like domains with the G764S and E769K mutations were significantly lower than the WT protein both in the absence and presence of calcium. This indicates that these mutations do affect the stability of the CaM-like domain although, given the high thermal stability of this domain, the importance of this destabilization at physiological temperatures is not clear. Similar to the WT CaM-

This article is protected by copyright. All rights reserved.

like domain, a statistically significant increase in T_m was seen for all three mutant proteins (R752Q, G764S and E769K) in the presence of calcium, indicating that they are able to bind and be stabilised by bound calcium ions. For the R752Q mutant the magnitude of this shift was similar to the WT at approximately 10°C, whereas for the G764S and E769K mutants it was somewhat less at 8 and 4°C respectively. This comparatively smaller shift is suggestive of less structural stabilisation due to sub-optimal calcium binding and would fit with the location of the G764S and E769K mutations immediately adjacent to the calcium co-ordinating residues in EF1 (Supplemental Fig. 1B).

Assessing calcium binding more quantitatively by isothermal calorimetry, we found that the WT CaM-like domain demonstrated a single binding event and a dissociation constant (114.94 ± 15.20 μM) in line previous reports [6,37]. Similar average K_d values were calculated for the R752Q and G764S, albeit with greater variance in the data obtained for these mutants. By contrast, binding efficiency appeared to be compromised in the E769K mutant for which DP and ΔH values were 10-fold lower then WT or other mutants. This precluded the accurate calculation of a K_d value but suggests a significant deficiency in calcium binding for this mutant. However, the high protein concentrations required for calorimetry experiments must be borne in mind as they may exacerbate changes in protein stability that might not be so significant under conditions of more physiological protein concentrations.

In actin bundling assays full-length actinin-1 proteins harbouring these mutations all bundled actin more efficiently than the WT protein and this bundling was reduced in the presence of calcium, indicating that all the CaM-like domain mutant proteins retain their calcium-sensitivity in this context. Cytoskeletal association of the G764S and E769K mutants in HeLa cells was also significantly enhanced, and all three mutants co-localized with actin filaments in both HeLa and differentiating MEG-01 megakaryoblast cells. Overall our data on the CaM-like domain mutations indicates that the E769K mutation has the greatest impact on protein stability and affects, but does not abolish, calcium binding, whereas R752Q and G764S mutant proteins appear to be minimally affected in this regard. In addition, enhanced bundling of and/or association with actin filaments is seen for all the three mutant proteins.

This article is protected by copyright. All rights reserved.

Accepted Article

Accepted Article

Calcium-sensitive regulation of actin by actinin-1 and other proteins is relevant to key aspects of platelet function including platelet activation when intracellular calcium concentration doubles [43] and plays a role in driving dramatic changes in cell shape [44]. Given the mild phenotype and normal platelet activation reported for patients with actinin-1 associated CMTP, it is perhaps unsurprising that calcium-binding efficiency is not dramatically affected by the reported CaM-like domain mutations, as the loss of calcium regulation of actinin-1 would likely have severe consequences for platelet function and for other actinin-1 expressing cells [11,12].

Rod domain mutations

A cluster of CMTP-linked mutations map to amino acids 737 and 738 that lie at the end of the last alpha helix of the 4th SR of the rod domain. Four families with either T737N or T737S mutations and eight families with R738W or R738Q mutations have been reported [8,11,12,15,16]. Interestingly the T737S mutation was classified as a variant of uncertain significance presumably due to, (1) its occurrence in a single family, (2) it being a relatively conservative substitution with low scores for its disruptive potential according to predictive bioinformatics algorithms and, (3) the lack of observed disruption of the actin cytoskeleton in cells transfected with actinin-1 harbouring this mutation [8]. In the crystal structure of actinin-2 EF1-2 lies on top of and is in close contact with SR4 and the residues equivalent to T737 and R738 are close to this interface (Supplemental Fig. 1C) [1]. Mutations of these residues in actinin-1 may thus affect the interaction of SR4 with the CaM-like domain and alter its regulation of actin binding. However, in the actinin-2 structure, while the equivalent threonine residue forms hydrogen bonds with residues from EF-2, the arginine side chain projects away from EF-2, not making close contact with the CaM-like domain. Perhaps reflecting this, we find here that both the T737N and T737S mutations potently increased actinin-1's ability to bundle actin filaments in vitro, whereas actinin-1 R738W shows only a slight increase in bundling activity that is not statistically significant (in agreement with our previous findings that showed a slight but not significant increase in cytoskeletal association for this mutant [20]). These findings indicate that the T737S mutation has functional consequences, supporting the case for it being classified as a likely pathogenic mutation and also suggest that bundling assays may be a useful quantitative method to assess the functional implications of actinin-1 mutations.

This article is protected by copyright. All rights reserved.

Accepted Article

In contrast to this cluster of mutations at the end of SR4, the R320Q, L395Q and L547P rod domain mutations that we examined are located some distance from the ABD and CaM-like domains (Supplemental Fig. 1D, 1E). Based on the actinin-2 structure, R320 lies close to the dimer interface whereas L395 and L547 do not. Nevertheless, all three mutant proteins elute as dimers from a gel filtration column (data not shown), and can bundle actin filaments, indicating that dimerization of the rod domain is not disrupted. The R320Q and L395Q mutant proteins have dramatically increased actin bundling ability *in vitro* whereas actin bundling for L547P was not significantly increased compared to WT actinin-1. The L395Q mutation maps to the first helix of SR2 in the middle of rod domain and in the actinin-2 structure the equivalent leucine residue is facing away from the dimer interface with its sidechain projecting towards helix 2 of SR2 (Supplemental Fig. 1D-E). The R320Q mutation maps to helix 2 of SR1. The sidechain of the equivalent arginine residue in actinin-2 makes polar contacts with three glutamate residues, one located in SR4 of the other actinin subunit and two located in helix 3 of SR1 (Supplemental Fig. 1F). Notably, helix 3 of SR1 continues as an unbroken alpha helix to become helix 1 of SR2. Thus, mutations such as R320Q and L395Q may be able to exert long distance effects through the long α-helices of the spectrin repeats, thereby influencing the CaM-like domain's regulation of actin binding and bundling. Our current understanding of actin filament cross linking by actinin indicates that the 90 degree twist present within the rod domain is not compatible with the tight bundling of actin filaments in a parallel or anti-parallel orientation [1,3,6]. Such bundling of filaments into tight fibres probably requires dissociation of EF3-4 from the neck region to give this region the conformational flexibility required to re-orient the ABD appropriately [1]. It is conceivable then that mutations in the rod domain may influence the bundling of actin filaments either by altering the twist of the rod domain, or by long range structural effects that influence the "clamping" of the neck region by EF3-4. A structure of the full-length actinin-1 dimer would greatly aid our understanding in this regard.

Yasutomi *et al* [10] reported that CHO cells expressing actinin-1 L395Q exhibited disorganization of the actin cytoskeleton with shorter and thicker actin fibres and similar effects have previously been reported for other CMTP-linked actinin-1 mutations [8,11–13] and most recently for eleven newly identified mutations (including nine in the rod domain) [17]. We found that actinin-1 L395Q association with the cytoskeleton in cultured HeLa cells appears similar to that of WT actinin-1 in contrast to the CaM-like domain mutations G764S and E769K. In addition, we did not observe notable cytoskeletal disruption, nor increased actin fibre diameter in HeLa cells for L395Q or the other mutations that we examined. Thus, it appears that the relationship between actin bundling

This article is protected by copyright. All rights reserved.

properties *in vitro* and actin association/organization *in-cellula* is not straightforward and is likely to be cell line-specific. We attempted to use differentiating MEG-01 megakaryoblast cells as a more relevant cellular model (Supplemental Fig. 2), but a high degree of intrinsic morphological heterogeneity in these cells complicated any analysis of the effects of transfected actinin-1 proteins. Primary cultures of rodent megakaryocytes are likely to be a better model to examine the mechanisms by which actinin-1 mutations affect platelet production.

In summary, all the CaM-like and rod domain actinin-1 mutants assessed here show varying degrees of increased association with F-actin *in vitro* and/or *in vivo*. This phenotype was demonstrated previously for several CMTP-causing mutations in the actinin-1 ABD [20]. A common mechanism thus appears to exist in the pathogenesis of actinin-1 related CMTP, regardless of the functional domain of actinin-1 affected. We hypothesise that some event(s) during platelet production, such as the extension of proplatelet shafts from megakaryocytes or the fission of large pre-platelets into mature platelets in the vasculature, may be exquisitely sensitive to a slightly increased affinity or bundling activity of actinin-1 for F-actin such that the CMTP-linked mutations affect platelets in the absence of any apparent phenotype in other tissues [45,46]. At the same time we cannot exclude the possibility that some of the CMTP-linked mutations might disrupt other protein: protein interactions that are essential for platelet formation, particularly given the many interacting proteins known to associate with the actinin-1 rod and other functional domains [47].

Authors' contributions

L.O'S., A.P.A. and K.M.D conducted the experiments presented in the manuscript. L.O'S., A.P.A., A.M. and E.G. generated expression constructs required for the study. P.W.Y. and L.O'S. analysed the data and co-wrote the manuscript.

Acknowledgements

We thank Caitriona O'Driscoll for providing access to the isothermal calorimetry instrument and Michael Cronin and Tania Hidalgo Crespo for their assistance and advice in relation to isothermal calorimetry experiments. We are grateful to Julia Samson for help with establishing the thermal shift assays. We acknowledge the Irish Research Council for their support of our work on actinins through a Government of Ireland Postgraduate Scholarship

This article is protected by copyright. All rights reserved.

Accepted Article

to LO'S (Project ID: GOIPG/2017/952), as well as the University College Cork, Translational Research Access Programme.

Accepted Article

References

1 Ribeiro E de A, Pinotsis N, Ghisleni A, Salmazo A, Konarev P V, Kostan J, Sjöblom B, Schreiner C, Polyansky AA, Gkougkoulia EA, Holt MR, Aachmann FL, Zagrović B, Bordignon E, Pirker KF, Svergun DI, Gautel M, Djinović-Carugo K & Djinović-Carugo K (2014) The structure and regulation of human muscle α-actinin. *Cell* **159**, 1447–60.

2 Blanchard A, Ohanian V & Critchley D (1989) The structure and function of α-actinin. *J. Muscle Res. Cell Motil.* **10**, 280–289.

3 Ylänne J, Scheffzek K, Young P & Saraste M (2001) Crystal structure of the alpha-actinin rod reveals an extensive torsional twist. *Structure* **9**, 597–604.

4 Kao H-Y, Zhang C, Wan P, Pasha Z, Guaiquil V, Liu A, Liu J, Luo Y, Fuchs E & Rosenblatt MI (2015) The actinin family proteins: biological function and clinical implications. *Cell Biosci.* **5**, 48.

5 Foley KS & Young PW (2014) The non-muscle functions of actinins: an update. *Biochem. J.* **459**, 1–13.

6 Prebil SD, Slapšak U, Pavšič M, Ilc G, Puž V, Ribeiro E de A, Anrather D, Hartl M, Backman L, Plavec J, Lenarčič B & Djinović-Carugo K (2016) Structure and calcium-binding studies of calmodulin-like domain of human non-muscle α-actinin-1. *Sci. Rep.* **6**, 27383.

7 Kunishima S & Saito H (2006) Congenital macrothrombocytopenias. *Blood Rev.* **20**, 111–121.

8 Faleschini M, Melazzini F, Marconi C, Giangregorio T, Pippucci T, Cigalini E, Pecci A, Bottega R, Ramenghi U, Siitonen T, Seri M, Pastore A, Savoia A & Noris P (2018) ACTN1 mutations lead to a benign form of platelet macrocytosis not always associated with thrombocytopenia. *Br. J. Haematol.* **183**, 276–288.

9 Westbury SK, Shoemark DK & Mumford AD (2017) *ACTN1* variants associated with thrombocytopenia. *Platelets* **28**, 625–627.

This article is protected by copyright. All rights reserved.

Accepted Article

10 Yasutomi M, Kunishima S, Okazaki S, Tanizawa A, Tsuchida S & Ohshima Y (2015) ACTN1 rod domain mutation associated with congenital macrothrombocytopenia. *Ann. Hematol.* **95**, 141–144.

11 Bottega R, Marconi C, Faleschini M, Baj G, Cagioni C, Pecci A, Pippucci T, Ramenghi U, Pardini S, Ngu L, Baronci C, Kunishima S, Balduini CL, Seri M, Savoia A & Noris P (2014) ACTN1-related thrombocytopenia: identification of novel families for phenotypic characterization. *Blood* **125**, 869–872.

12 Kunishima S, Okuno Y, Yoshida K, Shiraishi Y, Sanada M, Muramatsu H, Chiba K, Tanaka H, Miyazaki K, Sakai M, Ohtake M, Kobayashi R, Iguchi A, Niimi G, Otsu M, Takahashi Y, Miyano S, Saito H, Kojima S & Ogawa S (2013) ACTN1 mutations cause congenital macrothrombocytopenia. *Am. J. Hum. Genet.* **92**, 431–438.

13 Guéguen P, Rouault K, Chen JM, Raguénès O, Fichou Y, Hardy E, Gobin E, Pan-petesch B, Kerbiriou M, Trouvé P, Marcorelles P, Abgrall J francois, Le Maréchal C & Férec C (2013) A Missense Mutation in the Alpha-Actinin 1 Gene (ACTN1) Is the Cause of Autosomal Dominant Macrothrombocytopenia in a Large French Family. *PLoS One* **8**, 1–8.

14 Johnson B, Lowe GC, Futterer J, Lordkipanidze M, MacDonald D, Simpson MA, Sanchez-Guiu I, Drake S, Bem D, Leo V, Fletcher SJ, Dawood B, Rivera J, Allsup D, Biss T, Bolton-Maggs PH, Collins P, Curry N, Grimley C, James B, Makris M, Motwani J, Pavord S, Talks K, Thachil J, Wilde J, Williams M, Harrison P, Gissen P, Mundell S, Mumford A, Daly ME, Watson SP & Morgan N V (2016) Whole exome sequencing identifies genetic variants in inherited thrombocytopenia with secondary qualitative function defects. *Haematologica* **101**, 1170–1179.

15 Boutroux H, David B, Guéguen P, Frange P, Vincenot A, Leverger G & Favier R (2017) ACTN1-related Macrothrombocytopenia: A Novel Entity in the Progressing Field of Pediatric Thrombocytopenia. *J. Pediatr. Hematol. Oncol.*, 28562514.

16 Westbury SK, Turro E, Greene D, Lentaigne C, Kelly AM, Bariana TK, Simeoni I, Pillois X, Attwood A, Austin S, Jansen SBG, Bakchoul T, Crisp-Hihn A, Erber WN, Favier R, Foad N, Gattens M, Jolley JD, Liesner R, Meacham S, Millar CM, Nurden AT, Peerlinck K, Perry DJ, Poudel P, Schulman S, Schulze H, Stephens JC, Furie B, Robinson PN, van Geet C, Rendon A, Gomez K, Laffan MA, Lambert MP, Nurden P, Ouwehand WH, Richardson S, Mumford AD & Freson K (2015) Human phenotype ontology annotation and cluster analysis to unravel genetic defects in 707 cases with unexplained bleeding and platelet disorders. *Genome Med.* **7**.

This article is protected by copyright. All rights reserved.

Accepted Article

17 Vincenot A et al. (2019) Novel ACTN1 variants in cases of thrombocytopenia. *Hum. Mutat.*

18 Murphy ACH & Young PW (2015) The actinin family of actin cross-linking proteins - A genetic perspective. *Cell Biosci.* **5**, 1–9.

19 Feng D, Notbohm J, Benjamin A, He S, Wang M, Ang L-H, Bantawa M, Bouzid M, Del Gado E, Krishnan R & Pollak MR (2018) Disease-causing mutation in α-actinin-4 promotes podocyte detachment through maladaptation to periodic stretch. *Proc. Natl. Acad. Sci. U. S. A.* **115**, 1517–1522.

20 Murphy ACH, Lindsay AJ, McCaffrey MW, Djinovic-Carugo K & Young PW (2016) Congenital macrothrombocytopenia-linked mutations in the actin-binding domain of alpha-actinin-1 enhance F-actin association. *FEBS Lett.* **590**, 685–695.

21 Rosenberg S, Stracher a & Burridge K (1981) Isolation and characterization of a calcium-sensitive alpha-actinin-like protein from human platelet cytoskeletons. *J. Biol. Chem.* **256**, 12986–91.

22 Landon F & Olomucki A (1983) Isolation and physico-chemical properties of blood platelet alpha-actinin. *Biochim. Biophys. Acta* **742**, 129–34.

23 Astle WJ, Elding H, Jiang T, Allen D, Ruklisa D, Mann AL, Mead D, Bouman H, Riveros-Mckay F, Kostadima MA, Lambourne JJ, Sivapalaratnam S, Downes K, Kundu K, Bomba L, Berentsen K, Bradley JR, Daugherty LC, Delaneau O, Freson K, Garner SF, Grassi L, Guerrero J, Haimel M, Janssen-Megens EM, Kaan A, Kamat M, Kim B, Mandoli A, Marchini J, Martens JHA, Meacham S, Megy K, O'Connell J, Petersen R, Sharifi N, Sheard SM, Staley JR, Tuna S, van der Ent M, Walter K, Wang SY, Wheeler E, Wilder SP, Iotchkova V, Moore C, Sambrook J, Stunnenberg HG, Di Angelantonio E, Kaptoge S, Kuijpers TW, Carrillo-de-Santa-Pau E, Juan D, Rico D, Valencia A, Chen L, Ge B, Vasquez L, Kwan T, Garrido-Martín D, Watt S, Yang Y, Guigo R, Beck S, Paul DS, Pastinen T, Bujold D, Bourque G, Frontini M, Danesh J, Roberts DJ, Ouwehand WH, Butterworth AS & Soranzo N (2016) The Allelic Landscape of Human Blood Cell Trait Variation and Links to Common Complex Disease. *Cell* **167**, 1415-1429.e19.

24 Schick UM, Jain D, Hodonsky CJ, Morrison J V., Davis JP, Brown L, Sofer T, Conomos MP, Schurmann C, McHugh CP, Nelson SC, Vadlamudi S, Stilp A, Plantinga A, Baier L, Bien SA, Gogarten SM, Laurie CA, Taylor KD, Liu Y, Auer PL, Franceschini N, Szpiro A, Rice K, Kerr KF, Rotter JI, Hanson RL, Papanicolaou G, Rich SS, Loos RJF, Browning BL, Browning SR, Weir BS, Laurie CC, Mohlke KL, North KE, Thornton TA & Reiner AP (2016) Genome-wide Association Study of Platelet Count Identifies Ancestry-Specific Loci in Hispanic/Latino Americans. *Am. J.*

This article is protected by copyright. All rights reserved.

Hum. Genet. **98**, 229–242.

25 Gieger C, Radhakrishnan A, Cvejic A, Tang W, Porcu E, Pistis G, Serbanovic-Canic J, Elling U, Goodall AH, Labrune Y, Lopez LM, Mägi R, Meacham S, Okada Y, Pirastu N, Sorice R, Teumer A, Voss K, Zhang W, Ramirez-Solis R, Bis JC, Ellinghaus D, Gögele M, Hottenga J-J, Langenberg C, Kovacs P, O'Reilly PF, Shin S-Y, Esko T, Hartiala J, Kanoni S, Murgia F, Parsa A, Stephens J, van der Harst P, Ellen van der Schoot C, Allayee H, Attwood A, Balkau B, Bastardot F, Basu S, Baumeister SE, Biino G, Bomba L, Bonnefond A, Cambien F, Chambers JC, Cucca F, D'Adamo P, Davies G, de Boer RA, de Geus EJC, Döring A, Elliott P, Erdmann J, Evans DM, Falchi M, Feng W, Folsom AR, Frazer IH, Gibson QD, Glazer NL, Hammond C, Hartikainen A-L, Heckbert SR, Hengstenberg C, Hersch M, Illig T, Loos RJF, Jolley J, Khaw K-T, Kühnel B, Kyrtsonis M-C, Lagou V, Lloyd-Jones H, Lumley T, Mangino M, Maschio A, Mateo Leach I, McKnight B, Memari Y, Mitchell BD, Montgomery GW, Nakamura Y, Nauck M, Navis G, Nöthlings U, Nolte IM, Porteous DJ, Pouta A, Pramstaller PP, Pullat J, Ring SM, Rotter JI, Ruggiero D, Ruokonen A, Sala C, Samani NJ, Sambrook J, Schlessinger D, Schreiber S, Schunkert H, Scott J, Smith NL, Snieder H, Starr JM, Stumvoll M, Takahashi A, Wilson Tang WH, Taylor K, Tenesa A, Lay Thein S, Tönjes A, Uda M, Ulivi S, van Veldhuisen DJ, Visscher PM, Völker U, Wichmann H-E, Wiggins KL, Willemsen G, Yang T-P, Hua Zhao J, Zitting P, Bradley JR, Dedoussis G V., Gasparini P, Hazen SL, Metspalu A, Pirastu M, Shuldiner AR, Joost van Pelt L, Zwaginga J-J, Boomsma DI, Deary IJ, Franke A, Froguel P, Ganesh SK, Jarvelin M-R, Martin NG, Meisinger C, Psaty BM, Spector TD, Wareham NJ, Akkerman J-WN, Ciullo M, Deloukas P, Greinacher A, Jupe S, Kamatani N, Khadake J, Kooner JS, Penninger J, Prokopenko I, Stemple D, Toniolo D, Wernisch L, Sanna S, Hicks AA, Rendon A, Ferreira MA, Ouwehand WH & Soranzo N (2011) New gene functions in megakaryopoiesis and platelet formation. *Nature* **480**, 201–208.

26 Dessen P, Le Roux DT, Kauffmann A, Robert T, Larbret F, Sekkai D, Ripoche H, Debili N, Lazar V, Kroemer G, Vainchenker W & Raslova H (2006) Interrelation between polyploidization and megakaryocyte differentiation: a gene profiling approach. *Blood* **109**, 3225–3234.

27 Elagib KE, Rubinstein JD, Delehanty LL, Ngoh VS, Greer PA, Li S, Lee JK, Li Z, Orkin SH, Mihaylov IS & Goldfarb AN (2013) Calpain 2 activation of P-TEFb drives megakaryocyte morphogenesis and is disrupted by leukemogenic GATA1 mutation. *Dev. Cell* **27**, 607–620.

28 Machlus KR, Thon JN & Italiano JE (2014) Interpreting the developmental dance of the megakaryocyte: A review of the cellular and molecular processes mediating platelet formation. *Br. J. Haematol.* **165**, 227–236.

This article is protected by copyright. All rights reserved.

Accepted Article

Accepted Article

29 Otey CA, Vasquez GB, Burridge K & Erickson BW (1993) Mapping of the ??-actinin binding site within the ??1 integrin cytoplasmic domain. *J. Biol. Chem.* **268**, 21193–21197.

30 Izaguirre G, Aguirre L, Ji P, Aneskievich B & Haimovich B (1999) Tyrosine phosphorylation of alpha-actinin in activated platelets. *J. Biol. Chem.* **274**, 37012–20.

31 Feng S, Reséndiz JC, Christodoulides N, Lu X, Arboleda D, Berndt MC & Kroll MH (2002) Pathological shear stress stimulates the tyrosine phosphorylation of alpha-actinin associated with the glycoprotein Ib-IX complex. *Biochemistry* **41**, 1100–8.

32 Reséndiz JC, Feng S, Ji G & Kroll MH (2004) von Willebrand factor binding to platelet glycoprotein Ib-IX-V stimulates the assembly of an alpha-actinin-based signaling complex. *J. Thromb. Haemost.* **2**, 161–9.

33 Tadokoro S, Nakazawa T, Kamae T, Kiyomizu K, Kashiwagi H, Honda S, Kanakura Y & Tomiyama Y (2011) Apotential role for α-actinin in inside-out αIIbβ3 signaling. *Blood* **117**, 250–258.

34 Foley KS & Young PW (2013) An analysis of splicing, actin-binding properties, heterodimerization and molecular interactions of the non-muscle α-actinins. *Biochem. J.* **452**, 477–488.

35 Choi S, Kelber J, Jiang X, Strnadel J, Fujimura K, Pasillas M, Coppinger J & Klemke R (2014) Procedures for the biochemical enrichment and proteomic analysis of the cytoskeletome. *Anal. Biochem.* **446**, 102–7.

36 Rasband WS ImageJ, U. S. National Institutes of Health, Bethesda, Maryland, USA. .

37 Backman L (2015) Calcium affinity of human α-actinin 1. *PeerJ* **3**, e944.

38 Bottega R, Marconi C, Faleschini M, Baj G, Cagioni C, Pecci A, Pippucci T, Ramenghi U, Pardini S, Ngu L, Baronci C, Kunishima S, Balduini CL, Seri M, Savoia A & Noris P (2015) ACTN1 -related thrombocytopenia : identi fi cation of novel families for phenotypic characterization. **125**, 869–873.

39 Crowther GJ, He P, Rodenbough PP, Thomas AP, Kovzun K V, Leibly DJ, Bhandari J, Castaneda LJ, Hol WGJ, Gelb MH, Napuli AJ & Van Voorhis WC (2010) Use of thermal melt curves to assess the quality of enzyme preparations. *Anal. Biochem.* **399**, 268–75.

40 Huynh K & Partch CL (2015) Analysis of protein stability and ligand interactions by thermal shift assay. *Curr. Protoc. Protein Sci.* **2015**, 19.26.1-19.26.14.

41 Brzeska H, Venyaminov SV, Grabarek Z & Drabikowski W (1983) *Comparative studies on*

This article is protected by copyright. All rights reserved.

thermostability of calmodulin, skeletal muscle troponin C and their tryptic fragments.

42 Wendt B, Hofmann T, Martin SR, Bayley P, Brodin P, Grundstrom T, Thulin E, Linse S & Forsen S (1988) Effect of amino acid substitutions and deletions on the thermal stability, the pH stability and unfolding by urea of bovine calbindin D9k. *FEBS* **175**, 439–445.

43 Oliver AE, Tablin F, Walker NJ & Crowe JH (1999) The internal calcium concentration of human platelets increases during chilling. *Biochim. Biophys. Acta - Biomembr.* **1416**, 349–360.

44 Gupta S, Donati A & Reviakine I (2016) Differences in intracellular calcium dynamics cause differences in α-granule secretion and phosphatidylserine expression in platelets adhering on glass and TiO_2. *Biointerphases* **11**, 029807.

45 Thon JN, Montalvo A, Patel-Hett S, Devine MT, Richardson JL, Ehrlicher A, Larson MK, Hoffmeister K, Hartwig JH & Italiano JE (2010) Cytoskeletal mechanics of proplatelet maturation and platelet release. *J. Cell Biol.* **191**, 861–874.

46 Schwertz H, Köster S, Kahr WHA, Michetti N, Kraemer BF, Weitz DA, Blaylock RC, Kraiss LW, Greinacher A, Zimmerman GA & Weyrich AS (2010) Anucleate platelets generate progeny. *Blood* **115**, 3801–3809.

47 Djinovic-Carugo K, Gautel M, Ylänne J & Young P (2002) The spectrin repeat: A structural platform for cytoskeletal protein assemblies. *FEBS Lett.* **513**, 119–123.

48 Young P & Gautel M (2000) The interaction of titin and alpha-actinin is controlled by a phospholipid-regulated intramolecular pseudoligand mechanism. *EMBO J.* **19**, 6331–40.

Accepted Article

This article is protected by copyright. All rights reserved.

Tables

Table 1: Thermodynamic parameters obtained in the analysis of calcium binding efficiency in WT and mutant actinin-1 CaM-like domains by isothermal calorimetry.

Sample	n	Kd (µM)	N	ΔH	ΔG	TΔS
WT	3	114.94 ± 15.20	0.96 ± 0.15	1.97 ± 0.56	-5.38 ± 0.83	7.34 ± 0.48
R752Q	4	119.7 ± 80.29	0.81 ± 0.61	21.13 ± 39.25	-5.52 ± 0.56	26.64 ± 39.27
G764S	4	102.24 ± 67.64	1.53 ± 1.14	14.15 ± 26.17	-5.60 ± 0.53	6.8 ± 0.45

Accepted Article

This article is protected by copyright. All rights reserved.

Accepted Article

Figure Legends

Figure 1 : Location of amino acids that are mutated in CMTP within the actinin protein structure.

Domain organisation of the actinin-1 dimer showing the interaction of the CaM-like domain with the neck region of the opposing subunit that is thought to regulate actin binding [1,6,48]. The approximate positions of selected CMTP-linked mutations are indicated by arrows. Red arrows indicate the mutations in the rod and CaM-like (CaM) domains examined in this study, while black arrows represent mutations in the ABD that were previously shown to increase actinin-1 association with F-actin [20].

Figure 2 : Analysis of thermal stability and calcium binding of mutant actinin-1 CaM-like domains by thermal shift assay.

(A) Representative plots of fluorescence verses temperature for WT and mutant CaM-like domain proteins in the absence (dark grey) and presence of 1 mM $CaCl_2$ (light grey). High initial fluorescence was seen for all proteins, with typical melting profiles seen as the temperature rose above 60 °C.

(B) Average plots of melting profiles for all proteins (n = 7).

(C) Derivative plots of average data where the lowest points on the curve correspond to melting temperature.

(D) Analysis of melting temperatures in the absence and presence of calcium. All proteins exhibited increased thermal stability in the presence of calcium (significance level indicated above the brackets), while two mutants (G764S and E769K) had significantly lower melting temperatures than the WT protein under both conditions (significance level indicated above the error bars; n = 7; error bars represent SEM). Statistical analysis by One-Way ANOVA and post-hoc analysis by Dunnett's Test was used to compare WT and mutant protein melting temperatures. The paired sample T-Test was used to compare melting temperatures for each protein in the presence and absence of calcium. ** = ($P<0.01$), * = ($p<0.05$)

This article is protected by copyright. All rights reserved.

Accepted Article

Figure 3 : Calcium binding affinity of WT and mutant actinin-1 CaM-like domains assessed by isothermal calorimetry.

$CaCl_2$ was titrated against WT or the indicated mutant CaM-like domain proteins by injections of equal volume at regular time intervals. The top graph in each case shows the raw data as a function of time; the heat of the binding reaction is monitored as the differential power (DP) (µcal/s) required to maintain the experimental cell at the same temperature (25 °C) as the reference cell. The lower graph shows the processed data after normalization per mol of injectant, integration with respect to time and subtraction of reference data. The solid line is the calculated best fitting curve to this data obtained by optimization of the fitting parameters stoichiometry (n), enthalpy (ΔH) and dissociation constant (K_d) using the Microcal-PEAQ ITC software (Malvern Panalytical). Graphs shown are representative runs while the average values of these parameters obtained for each protein are shown in Table 1.

Figure 4 : Comparison of the actin bundling efficiency of WT and mutant actinin-1 proteins.

(A) Representative gels showing actin present in supernatant (S) and pellet (P) following bundling reaction in the presence of 0.2 mM EGTA or 0.1 mM $CaCl_2$ for WT and mutant actinin-1 proteins. WT (n=13) L395Q (n=9), R738W (n=7), R752Q (n=10), G764S (n=11) and E769K (n=8)

(B) Percentage actinin bound to actin in pellets in presence of 0.2 mM EGTA and 0.1 mM $CaCl_2$ for WT and mutant actinin-1 proteins. Bundling efficiency is reduced in presence of $CaCl_2$.

(C) Percentage actin bundled in bundling reactions shown in (A).

(D) Representative gels showing actin present in supernatant (S) and pellet (P) following bundling reaction in the presence of 0.2 mM EGTA for additional rod domain mutants. (n=3 for all samples)

(E) Percentage actinin bound to actin in pellets in the presence of 0.2 mM EGTA for additional rod domain mutants.

(F) Percentage actin bundled in the reactions shown in (D).

Quantification of results is presented as the mean ± SEM. Actin bundling and actinin binding by mutants was compared to WT using One-Way ANOVA and post-hoc analysis using

This article is protected by copyright. All rights reserved.

Dunnett's Test. Actin bundling and actinin binding for EGTA and $CaCl_2$ reactions were compared for all samples using a paired T-test for related samples. *P<0.05, **P<0.01.

Figure 5 : Cytoskeletal association of actinin-1 proteins with CMTP-associated mutations *in-cellula* and actin cytoskeletal organisation in HeLa and MEG-01 cells expressing GFP-tagged actinin-1 proteins with CMTP-associated mutations

(A) and (B) Cytosolic / nuclear and cytoskeletal fractions were prepared from HeLa cells transfected with FLAG-tagged WT or mutant actinin expression constructs. (A) Western blot analysis showing the levels of FLAG-actinin in each fraction as well as demonstrating successful fractionation as indicated by the detection of GAPDH primarily in the cytosolic / nuclear fraction. (B) Quantification of the amount of mutant FLAG-actinin relative to the WT protein in each fraction (normalized to actin levels). Proteins with the CaM-like domain mutations G764S and E769K are present in the cytoskeletal fraction at significantly greater higher levels as assessed by One-Way ANOVA and post-hoc Dunnett's Test. (** p<0.01, * p<0.05) (n=3)

(C) Expression of WT and mutant actinin-GFP proteins in HeLa cells. F-actin is stained with rhodamine phalloidin and actinin-1 proteins are detected through GFP fluorescence (red and green in merged images). The actin cytoskeleton does not appear disorganised in HeLa cells expressing mutant actinin-1 proteins, compared with cells expressing WT actinin-1 or neighbouring untransfected cells. GFP-tagged actinin-1 co-localises to a great extent with actin for both WT and mutant actinins. Scalebar represents 20 μm.

(D) Quantitative analysis of the width of actin fibres in HeLa cells transfected with WT or mutant actinin-GFP as indicated in (C). Statistical analysis of mean actin fibre width by One-Way ANOVA and post-hoc Dunnett's Test showed that variation between samples was non-significant.

Accepted Article

This article is protected by copyright. All rights reserved.

Accepted Article

Supplemental Figure 1 : Location of amino acids that are mutated in CMTP within the actinin protein structure

(A) Domain organisation of the actinin-1 dimer showing the interaction of the CaM-like domain with the neck region of the opposing subunit that is thought to regulate actin binding [1,6,48]. The approximate positions of selected CMTP-linked mutations are indicated by arrows. Red arrows indicate the mutations in the rod and CaM-like (CaM) domains examined in this study, while black arrows represent mutations in the ABD that were previously shown to increase actinin-1 association with F-actin [20].

(B) An NMR structure of the CaM-like domain of actinin-1 with calcium bound (PDB ID: 2N8Y [6]). Residues that are mutated in actinin-1-linked CMTP are highlighted in red, while those that co-ordinate the calcium ion (blue sphere) are coloured yellow (with side chains shown).

(C) The crystal structure of the full-length actinin-2 (PDB ID: 4D1E;[1]), highlighting the end of spectrin-like repeat 4 (SR4) of the rod domain and the CaM-like domain from one monomer and the ABD and neck region of the opposing monomer in the anti-parallel dimer. The residues within actinin-2 that are equivalent to the CMTP-linked mutations in actinin-1 are coloured red with side chains shown (T737 = T744, R738 = R745, R752 = R759, G764 = G771, E769 = E776).

(D,E,F) The crystal structure of the full-length actinin-2 (PDB ID: 4D1E;[1]), highlighting a region of the rod domain that includes parts of SR1 and 2 from one subunit (dark green) and SR3 and 4 from the other (light green). The residues within actinin-2 that are equivalent to the CMTP-linked mutations in central rod domain of actinin-1 are coloured red with side chains shown. D = surface representation, E = cartoon representation, F = magnified view of R327 showing polar contacts with three glutamate side chains (L395 = L402, R320 = R327, L547 = L554).

Images in B-F were prepared using the PyMOL Molecular Graphics System, Version 2.0 Schrödinger, LLC.

This article is protected by copyright. All rights reserved.

Accepted Article

Supplemental Figure 2: Expression of WT and mutant actinin-GFP proteins in MEG-01 cells

Although large variation in cell morphology and actin structure is observed between individual MEG-01 cells, GFP-tagged actinin-1 does appear to co-localise with F-actin, regardless of CMTP-associated mutations. Scalebar represents 20 µm.

Supplementary Materials & Methods

Actin co-sedimentation assays

Actin co-sedimentation assays were performed essentially as previously described [20,34]. Briefly, 2 µM of polymerized rabbit skeletal muscle actin (Cytoskeleton Inc., AKL99) was mixed with 1 µM purified full-length actinin in F-actin buffer (10 mM Tris-HCl pH 7.5, 100 mM NaCl, 10 mM NaN_3, 10 mM $MgCl_2$, 1 mM ATP, and 1 mM DTT) in the presence of 0.2 mM ethylene glycol-bis(2-aminoethylether) tetra-acetic acid (EGTA) for analysis of actinin in the calcium-unbound state or 0.1 mM $CaCl_2$ for analysis of actinin in the calcium-bound state. For all WT and mutant actinin proteins, a control actin-free reaction was carried out to account for artefactual sedimentation of actinin. One actin-only control was also carried out per experimental replicate and run on the same gel as experimental samples. Reactions, in a total volume of 100 µL, were incubated for 30 min at 30 ℃ and bundled actin was then pelleted by centrifugation at 16,000 x g at 30 ℃. Pellets and supernatants were analysed on SDS-polyacrylamide gels stained using GelCode™ BlueSafe Protein Stain (Thermo Scientific). Gels were imaged and bands were quantified using Odyssey Image Studio Software (LI-COR Biosciences). Sedimented actin in actinin-free control reaction and sedimented actinin in actin-free control reactions were subtracted from experimental reactions. Actin bundling, as well as the actin-binding ability of WT and mutant actinins in the presence and absence of calcium was determined by quantifying the percentage of actin or actinin sedimented in pellets of $CaCl_2$ and EGTA containing reactions respectively.

This article is protected by copyright. All rights reserved.

Accepted Article

Cytoskeletal purification assays

Purification of cytoskeletal fractions from HeLa cells was carried out largely as previously described [20,35]. HeLa cells (0.4 x 10^6 cells per plate) were plated on 6 cm dishes and grown for 24 hours at 37 ℃ in DMEM, 10% FBS, with Penicillin/Streptomycin media. At 24 hours, cells were 40 - 50% confluent and media was replaced with 1.7 mL antibiotic-free DMEM, 10% FBS media per plate. Cells were transfected with 2 µg of pCMV-NFLAG plasmid DNA encoding actinin-1 with an amino-terminal FLAG epitope tag and 0.5 µg pEGFP plasmid DNA that expresses green fluorescent protein as a transfection and fractionation control. DNA was suspended in 300 µL OptiMEM media and 2 µL Lipofectamine and added to 1.7 mL media per plate. Media was changed 16 hours post transfection and cytoskeletal purification was carried out 36 hours post-transfection. Media was removed and plates were placed on ice. Plates were washed twice in 800 µL PBS and washes were discarded. 200 µL lysis buffer (50 mM PIPES pH 6.9, 50 mM NaCl, 5% Glycerol, 0.1% NP-40, 0.1% Triton X-100, 0.1% Tween 20) was added to the plates on ice and the plates were rocked for 1.5 minutes before removing and retaining lysate. 800 µL wash buffer (50 mM Tris-HCl pH 7.5) was used to rinse plates on ice following lysis and this wash was discarded. The plates were removed from ice and 100 µL nuclease buffer (10 mM $MgCl_2$, 2 mM $CaCl_2$, 10 U/mL benzonase, 50 mM Tris-HCl pH 7.5) was added to the centre of each plate and allowed to flow to edges of plate. The nuclease buffer was allowed to incubate at room temperature for 10 minutes and was pipetted off and returned to the centre of plates at 2.5 minute intervals. The nuclease buffer was removed following incubation and retained. Lysis buffer was added back onto plates on ice (without any rinsing) and plates were rocked very gently for 0.5 minutes. The lysis buffer was then removed and added to the nuclease buffer and retained as the "cytosolic / nuclear fraction". The plates were then rinsed with 800 µL lysis buffer on ice and this rinse was discarded. The plates were then washed with 800 µL wash buffer three times on ice. The plates were then removed from ice and 100 µL 1% SDS was added and the "cytoskeletal fraction" was collected by pipetting. All fractions contained protease (Complete protease inhibitor cocktail (without EDTA) (Roche)) and phosphatase inhibitors (5 mM NaF and 2 mM Na_3VO_4). The cytosolic / nuclear fraction and cytoskeletal fraction were assessed by SDS-PAGE and western blotting. Fractionation efficiency was assessed by western blotting using an anti-GAPDH antibody (1:3000 - Sigma, G9545), and in some cases an anti-GFP antibody (1:1500 - Abcam, ab290), both of which were predominantly found in the cytosolic / nuclear fraction. Blotting using anti-β-actin antibody (1:3000 - Sigma, A5441) was used as a loading control. Stability of actin-actinin association was assessed by detection and quantification of FLAG-tagged actinin in both fractions by anti-FLAG antibody (1:1500 - Sigma, F3165). Detection was achieved using an Odyssey infrared imaging system for β-actin and enhanced chemiluminescent detection for FLAG, GAPDH and GFP.

This article is protected by copyright. All rights reserved.

Actin and FLAG signal was quantified using ImageJ [36] and Image Studio (LI-COR Biosciences) software respectively. FLAG signal was normalised to actin for all samples and all samples were expressed as a normalised ratio with respect to the WT sample of that run.

Immunofluorescence studies in the MEG-01 megakaryocyte cell line

MEG-01 (DSMZ, ACC 364) cells were grown in RPMI-1640, 10% FBS with Penicillin, Streptomycin media for 12 days with differentiation using phorbol 12-myristate 13-acetate (PMA) at 1 ng/mL on days 1-3 and 10 ng/mL on days 3-12, with a complete media change every 2-3 days. On day 10, media was changed to RPMI-1640, 10% FBS and 0.5 x 10^6 cells were plated on glass-bottomed dishes. Transfection was carried out using 1 µg Actinin-1-GFP plasmid with 1 µL Lipofectamine-2000 in 100 µL OptiMEM per dish in 1 mL of culture. On day 11, dishes were supplemented with an additional 1 mL of media. On day 12, media was removed, and adhered cells were fixed and stained as described for HeLa cells. Glass component of dishes were removed and mounted on coverslips as described for HeLa cells.

Accepted Article

This article is protected by copyright. All rights reserved.

Accepted Article

Figure 1

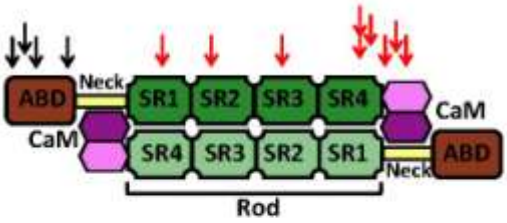

This article is protected by copyright. All rights reserved.

Accepted Article

Figure 2

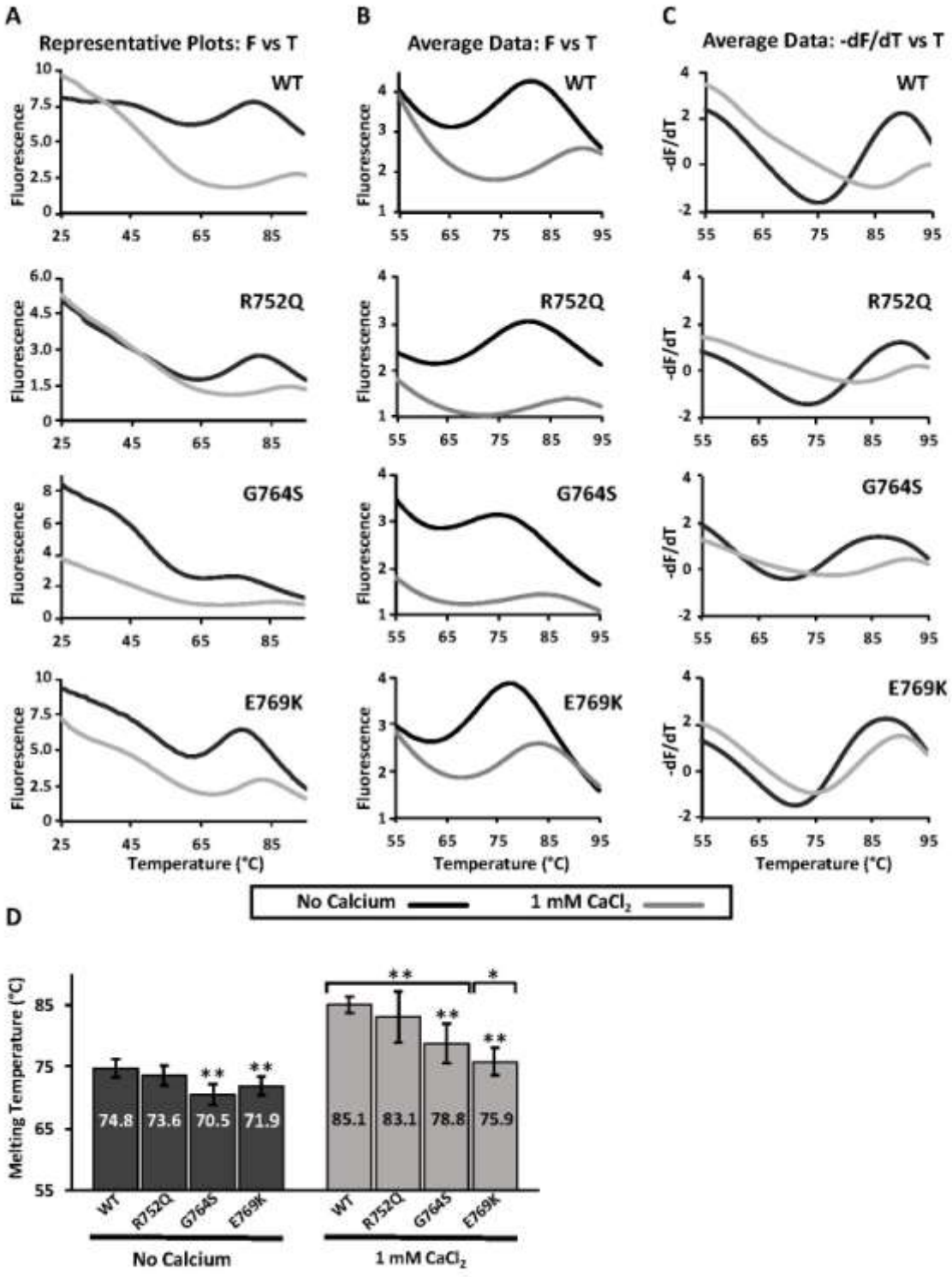

This article is protected by copyright. All rights reserved.

Accepted Article

Figure 3

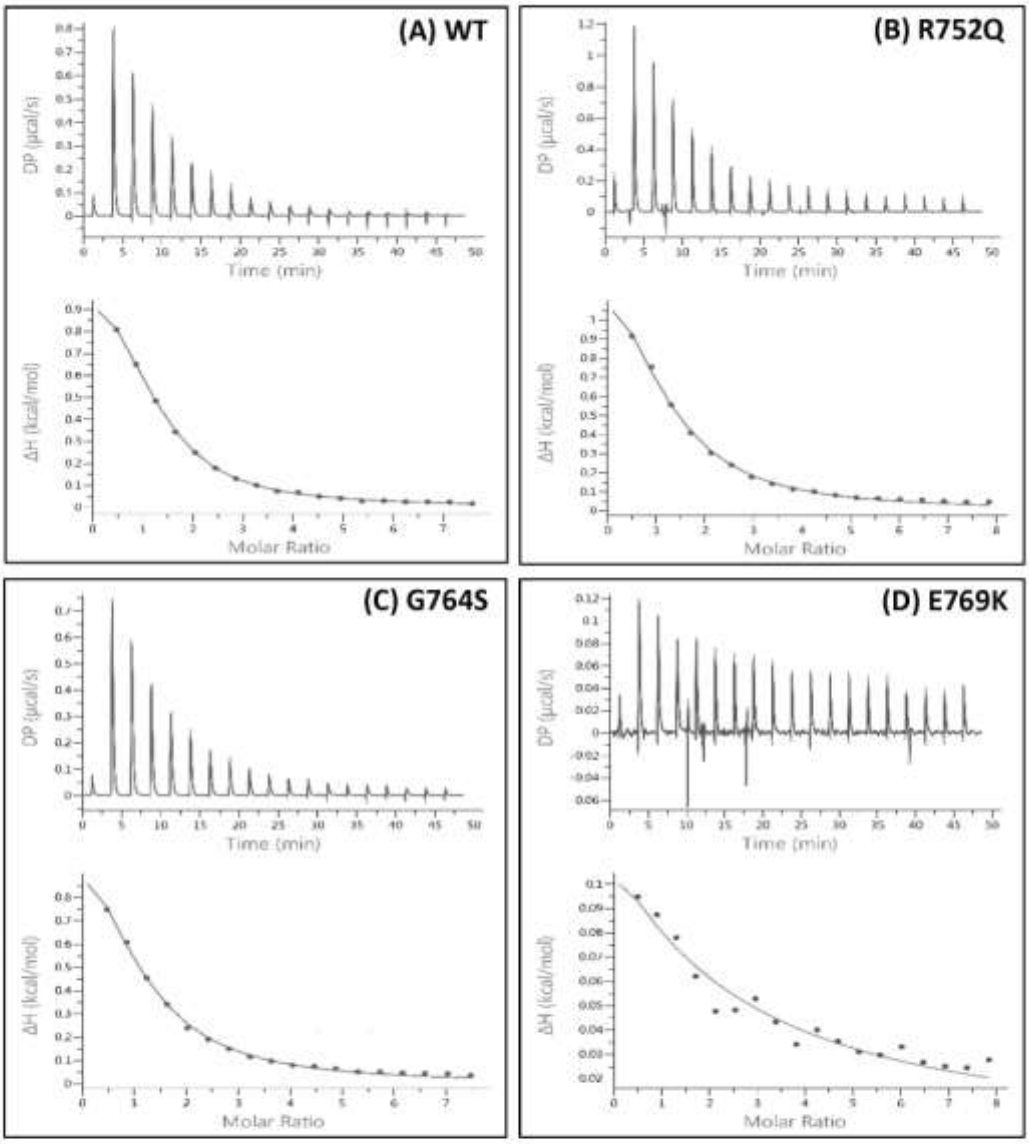

This article is protected by copyright. All rights reserved.

Accepted Article

Figure 4

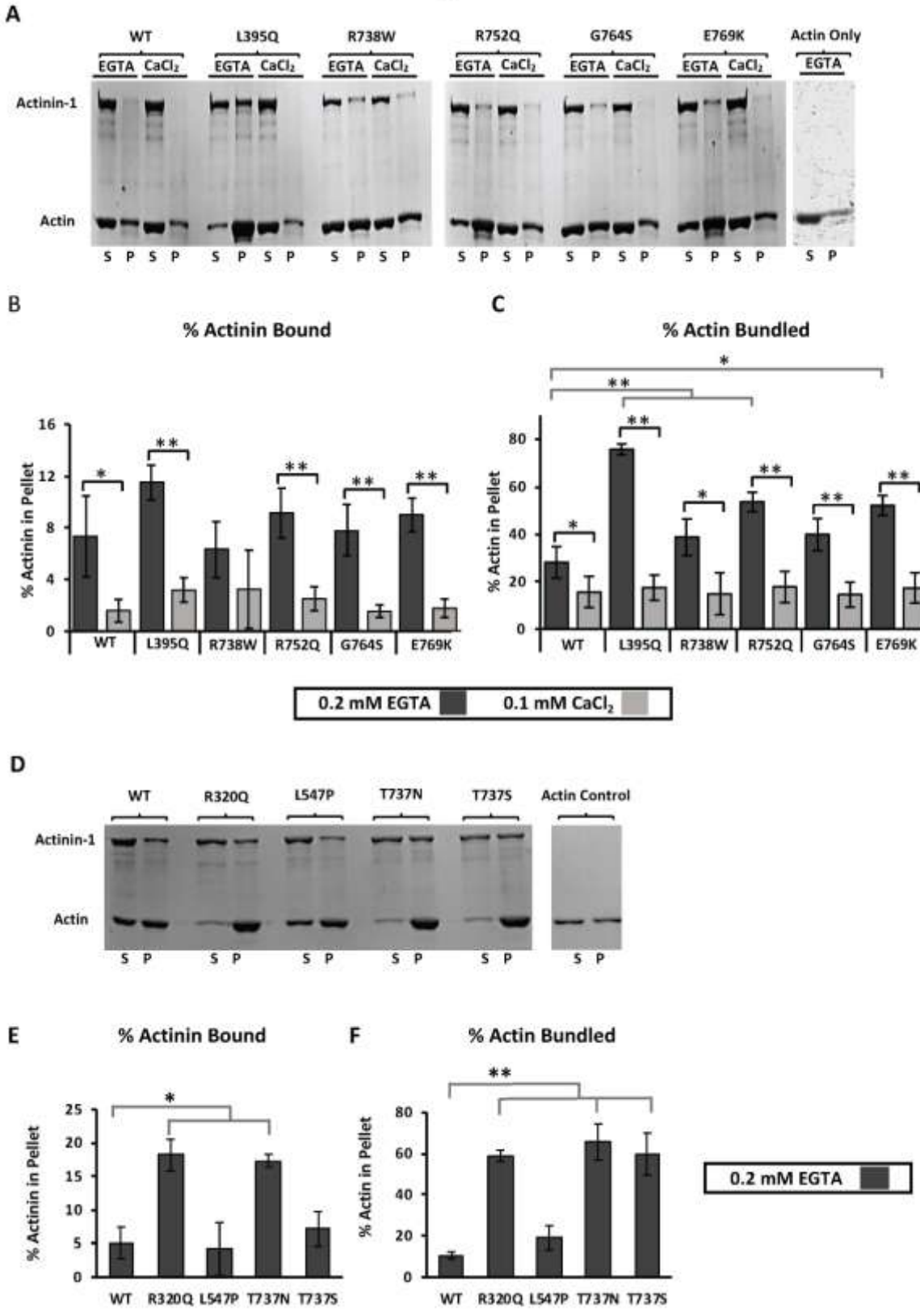

This article is protected by copyright. All rights reserved.

Accepted Article

Figure 5

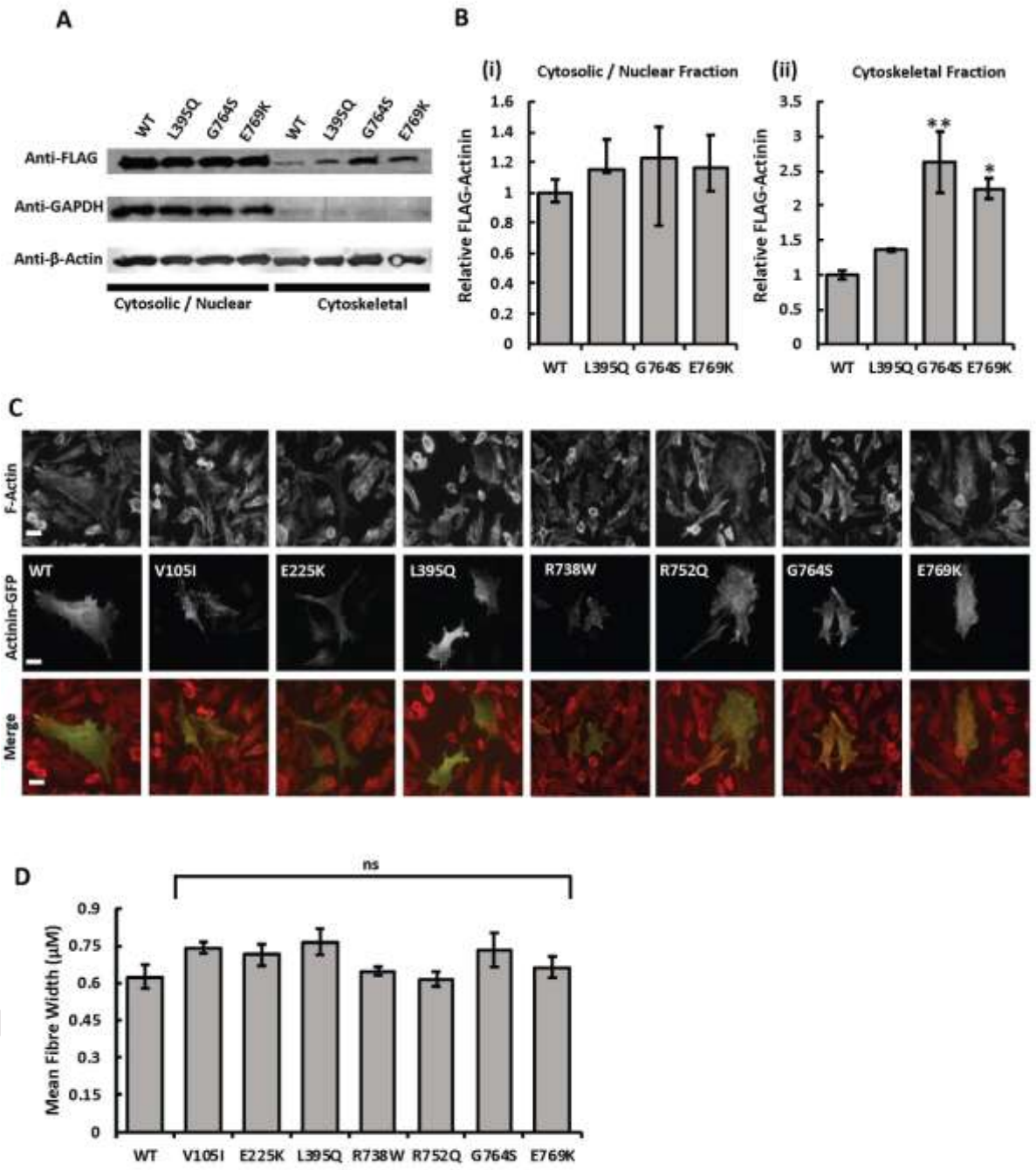

This article is protected by copyright. All rights reserved.